

UC Davis

UC Davis Previously Published Works

Title

Loss of Faap20 Causes Hematopoietic Stem and Progenitor Cell Depletion in Mice Under Genotoxic Stress

Permalink

<https://escholarship.org/uc/item/8774n57d>

Journal

Stem Cells, 33(7)

ISSN

1066-5099

Authors

Zhang, Tingting
Wilson, Andrew F
Mahmood Ali, Abdullah
[et al.](#)

Publication Date

2015-07-01

DOI

10.1002/stem.2048

Peer reviewed



Published in final edited form as:

Stem Cells. 2015 July ; 33(7): 2320–2330. doi:10.1002/stem.2048.

Loss of *Faap20* causes hematopoietic stem and progenitor cell depletion in mice under genotoxic stress

Tingting Zhang¹, Andrew F. Wilson¹, Abdullah Mahmood Ali¹, Satoshi H. Namekawa², Paul R. Andreassen¹, Amom Ruhikanta Meetei¹, and Qishen Pang¹

¹Division of Experimental Hematology and Cancer Biology, Cincinnati Children's Hospital Medical Center, Cincinnati, OH

²Division of Reproductive Sciences, Cincinnati Children's Hospital Medical Center, Cincinnati, OH

Abstract

FAAP20 is a recently identified protein that associates with the Fanconi anemia (FA) core complex component, FANCA. FAAP20 contains a conserved ubiquitin-binding zinc-finger domain, and plays critical roles in the FA-BRCA pathway of DNA repair and genome maintenance. The function of FAAP20 in animals has not been explored. Here we report that deletion of *Faap20* in mice led to a mild FA-like phenotype with defects in the reproductive and hematopoietic systems. Specifically, hematopoietic stem and progenitor cells (HSPCs) from *Faap20*^{-/-} mice showed defects in long-term multi-lineage reconstitution in lethally irradiated recipient mice, with milder phenotype as compared to HSPCs from *Fanca*^{-/-} or *Fancc*^{-/-} mice. *Faap20*^{-/-} mice are susceptible to mitomycin C (MMC)-induced pancytopenia. That is, acute MMC stress induced a significant progenitor loss especially the erythroid progenitors and megakaryocyte-erythrocyte progenitors (MEPs) in *Faap20*^{-/-} mice. Furthermore, *Faap20*^{-/-} HSPCs displayed aberrant cell cycle pattern during chronic MMC treatment. Finally, using *Faap20*^{-/-} *Fanca*^{-/-} double-knockout mice, we demonstrated a possible dominant effect of FANCA in the interaction between FAAP20 and FANCA. This novel *Faap20* mouse model may be valuable in studying the regulation of the FA pathway during bone marrow failure progress in FA patients.

Introduction

Fanconi anemia (FA) is a genetic disorder associated with congenital developmental defects, bone marrow failure and predisposition to cancers particularly acute myelogenous leukemia.¹⁻³ Complications of bone marrow failure and later myeloid malignancies are the major causes of the morbidity and mortality of FA patients.^{4,5} Loss of FA functions impairs

Address correspondence to: Qishen Pang, Division of Experimental Hematology and Cancer Biology, Cincinnati Children's Hospital Medical Center, 3333 Burnet Avenue, Cincinnati, Ohio 45229. Phone: (513) 636-1152. Fax: (513) 636-3768. Qishen.pang@cchmc.org..

Authorship

Contribution: T. Z., designed research, performed research, analyzed data and wrote the paper; A. F. W., performed research; A. M., performed research; S. H. N., contributed vital new reagents, designed research; P. R. A., contributed vital new reagents, designed research; A. R. M., contributed vital new reagents, designed research; Q. P., designed research and wrote the paper.

Conflict-of-interest disclosure: The authors declare no competing financial interests.

cellular responses to genotoxic and cytotoxic stresses, leading to hematopoietic failure and bone marrow failure in the early stage of FA.^{6,7} As a genetically heterogeneous disease, eight FA core complex proteins (FANCA, -B, -C, -E, -F, -G, -L, and -M), five associated factors (FAAP100, FAAP24, HES1, MHF1, and MHF2) and two mono-ubiquitination dimer proteins (FANCD2-FANCI) have been identified.⁸⁻¹⁰ All these proteins coordinate together in the FA pathway, facilitate DNA cross-link repair and cell-cycle control, thereby maintain the genome stability.^{8,9}

FAAP20 (20-kDa FANCA-associated Protein) was identified by several groups separately in the past two years as a novel integral subunit of the FA core complex. FAAP20 interacts with FANCA, an essential component of the FA core complex.¹¹⁻¹⁴ By stabilizing FANCA, FAAP20 modulates the ubiquitin ligase activity of the FA core complex, which is required for monoubiquitination of FANCD2. FAAP20 contains a conserved ubiquitin-binding zinc-finger domain (UBZ), which binds to monoubiquitinated form of Rev1 and promotes the interaction of the FA core complex with PCNA/Rev1 DNA damage bypass complexes.¹⁴ FAAP20 also binds to the ubiquitin product of RNF8-UBC13, recruits FA core complex to DNA Interstrand Cross Link site (ICLs) and promotes cellular resistance to ICLs.¹¹ Knockdown of FAAP20 in human somatic cells displays FA-like phenotypes.^{12,13} However, the function of FAAP20 in animals has not been explored.

In this report, we characterized a novel *Faap20* mouse model. We showed that deletion of *Faap20* in mice led to a mild FA-like phenotype compared to loss of the FA core complex. *Faap20*^{-/-} mice show defects in the reproductive system and are susceptible to mitomycin C (MMC)-induced bone marrow failure resulting from defects in early hematopoietic progenitor compartments.

Materials and Methods

Mice

Heterozygous *Faap20* mice in a C57BL/6 background were generated from the sperm purchased at the Knock-out Mice Program (KOMP) at the University of California Davis (Project ID# CSD23160). The IVF procedure was performed in Transgenic Animal and Genome Editing Core of Cincinnati Children's Hospital Medical Center. Heterozygotes *Faap20* mice were interbred to generate *Faap20* null mice and littermate controls. *Fanca*^{+/-} and *Fancc*^{+/-} mice were provided by Dr. Madeleine Carreau (Laval University) and Dr. Manuel Buchwald (Hospital for Sick Children, University of Toronto),^{15,16} respectively. Mice were maintained on C57BL/6 background in the animal barrier facility at Cincinnati Children's Hospital Medical Center. Animals were kept in accordance with the Institutional Animal Care and Use Committees (2C06040).

LacZ Tissue Histology

Briefly, E10.5-E11.5 embryos were harvested and placed in PBS, followed by fixation in 0.2% glutaraldehyde overnight at 4°C. The embryos were then incubated overnight at room temperature in the β -Gal staining solution (GALS kit, Sigma). For frozen section, the harvested tissues were prefixed in 0.2% glutaraldehyde overnight in 4°C. All samples were

transferred to a 30% sucrose PBS solution overnight. The samples were mounted in O.C.T mounting medium (Fisher Scientific), snap-frozen in isopentane/liquid nitrogen. Cryostat sectioning was performed and the 5mm thick sections were then stained with β -Gal solution (GALS kit, Sigma) for 4 hours at room temperature, and counterstained with Fast Red (N3020, Sigma).

Clonogenic survival assay

MEFs derived from different genotypes 11.5D embryos were treated with the indicated concentrations of MMC, then trypsinized and seeded in triplicate in 100-mm dishes at a density of 500 cells per dish. The cells were cultured in fresh medium for another 5-8 days. Colonies containing more than 50 cells were counted.

Flow cytometry

All the antibodies were obtained from eBioscience or BD Pharmingen unless otherwise indicated. Samples were examined on Fortessa or LSRII flow cytometry, and cytometry data were analyzed with BD FASC Diva or FlowJo software. For lineage cell analysis: Anti-CD71 and anti-Ter119 for erythroid, anti-Gr1 and anti-CD11b for granulocytic/monocytes, anti-CD45R (B220) for B-lymphoid, and anti-CD3e for T-lymphoid. For quantification of CMP, MEP, GMP, CLP, LK and LSK progenitors, mononucleated cell were separated by HISTOPAQUE 1083 (sigma) spin, then labeled with cocktail of anti-mouse lineage markers (CD3e, B220, Ter119, Mac1, and Gr1), anti-mouse CD117 (cKit), and anti-Ly-6A/E (Sca1), anti-CD34, anti-CD16/32, anti-CD150, anti-CD48 and anti-IL-7Ra. Common myeloid progenitors (CMPs) were defined as Lin-Sca1-cKit+CD34+ CD16/32low, and granulocyte-macrophage progenitors (GMPs) were defined as Lin-Sca1-cKit+CD34+CD16/32+. Megakaryocyte-erythroid progenitors (MEPs) were defined as Lin-Sca1-cKit+CD34-CD16/32-. Common lymphoid progenitors (CLPs) were defined as Lin-Sca1lowcKitlowIL-7Ra+, LK, LSK and SLAM cells were defined as Lin-Sca1-cKit+, Lin-Sca1+cKit+ and Lin-Sca1+cKit+CD48-CD150+, respectively (Fig. S4). Dead cells were excluded by 7-aminoactinomycin D staining (Sigma-Aldrich). FluoReporter lacZ Flow Cytometry Kit (F-1930, Life technologies) was used for the β -galactosidase activity flow cytometry quantification with fluorescein di-V-galactoside (FDG) in single cell. For cell cycle analysis, MEFs cells were fixed and permeabilized with Transcription Factor Buffer Set (BD Pharmingen), treated with 50ug/ml RNAase for 30 min at 37°C, then stained with Ki67 antibody (BD Pharmingen) and 10 mg/mL Propidium iodide (Sigma-Aldrich).

In vivo competitive repopulation assay

Briefly, bone marrow cells from different genotype mice were isolated and counted. Recipient CD45.1+ bone marrow cells were mixed with donor CD45.2+ bone marrow cells at a 1:1 ratio and then transplanted into lethally irradiated congenic C57BL/6 CD45.1+ recipient mice. Peripheral blood sample was collected through tail vein bleeding each month after transplantation. Mice were sacrificed 4 month later and subjected to bone marrow fraction analysis.

Hematopoietic colony assay

Bone marrow cells were isolated from femurs and tibiae of 6-8 weeks old mice, and 2×10^4 cells were put in 1 ml of Methocult M3434 media (StemCell Technologies) following standard protocols with or without MMC (sigma) treatment. Colonies were scored at day 10.

Hematology analysis

Peripheral blood was collected by tail vein bleeding. Measurements of the blood parameters were performed on a HEMAVET 950FS (Drew Scientific Group).

Western blot

FAAP20 protein expression was analyzed in homogenate tissue lysates by western blot using a polyclonal anti-C1orf86 isoform 2 (FAAP20) antibody (Sigma-Aldrich; HPA038829). Other antibody used in the experiments: anti-FANCD2 (Novus), anti-phospho-Histone H2A.X (Ser139) (Millipore), and anti-beta-actin (Sigma).

Statistical analysis

Student's t-test, ANOVA test, the Pearson's chi-square test were performed using Microsoft EXCEL software or Prism 6.0 software (GraphPad Software Inc). Error bars indicate SD. Differences were judged as significant if the P value was <0.05 (*), <0.01 (**) or <0.001 (***)

Results

Generation and characterization of *Faap20* mutant mice

To study the function of FAAP20, we generated *Faap20* knockout mice using sperm purchased from KOMP at UCSD (Project ID# CSD23160) and the knock in strategy was illustrated in Figure S1A. The *lacZ* knock-in allele allowed us to assess FAAP20 protein expression based on β -galactosidase activity in *Faap20*^{+/-} mice. We validated the knock-in and knock-out in the *Faap20* allele by genotyping using four sets PCR primers (Fig. S1B,C) and by Western blot analyzing with lysates from testes (Fig.S1D).

The offspring (n>200) from *Faap20*^{+/-} breeding followed predicted Mendelian frequencies, indicating no embryonic or perinatal lethality associated with *Faap20* knockout (Fig. S2A). No gross phenotypic differences were noted between the wild-type and *Faap20*^{-/-} offspring. The body weight of age- and sex-matched *Faap20*^{-/-} mice was similar to that of wild type littermates (Fig. S2B). Hematological parameters including WBC (white blood count), RBC (red blood count), Hb (Hb level) and PLT (platelet count) were grossly normal in 2 month-old *Faap20*^{-/-} mice comparing to wild type littermate controls (Fig. S2C).

Tissue specific FAAP20 protein expression in mice

We took advantage of *Faap20* promoter-driven *lacZ* transcription and examined *Faap20* expression in a developmental and tissue-specific manner. β -gal staining was observed in E11.5 of embryos development, with significantly higher expression in fetal liver, brain and

limbs than other tissues (Fig. S3A, B). In addition, intensive β -galactosidase staining was observed in brain, intestine, testis, ovary, and uterus tissues of 2 month-old *Faap20*^{+/-} mice (Fig. S3C). In contrast, *Faap20* expression was low in muscle, heart, kidney, lung, liver and spleen (Fig. S3C). We next examined tissue-specific *Faap20* expression by western blot. A strong 20-KDa band representing the mouse FAAP20 was detected from the lysates of testis, ovary, uterus, bone marrow and spleen of adult mice (Fig. S3D). This high level of *Faap20* expression in the testis, ovary, spleen and bone marrow suggests an indispensable role of *Faap20* in the reproductive and hematopoietic systems.

Reproductive defect in *Faap20*^{-/-} mice

Because *Faap20* was highly expressed in the testis and ovary, we evaluated reproductive performance of *Faap20*^{-/-} mice by monitoring the number of pups born per litter over time. We found that *Faap20*^{-/-} mice consistently produce small litters (Fig. 1A). In contrast, *Faap20* heterozygous mice did not show any defect in fertility (Fig. 1A). The size of the testes of 2 month-old *Faap20*^{-/-} mice was significantly smaller than those of wild-type littermate controls (Fig. 1B). Consistent with a smaller size, *Faap20*^{-/-} testes exhibited degenerated seminiferous tubules with decreased numbers of spermatocytes and spermatids (Fig. 1C). Histological analysis of ovaries from 2 month-old *Faap20*^{-/-} females also showed reduced ovarian size and markedly degenerated follicles (Fig. 1C).

To identify specific germ cell types that *Faap20* deletion likely affects the most, we examined *Faap20* expression in different cell populations of testis and ovary. β -Gal staining on the 2 month-old *Faap20*^{+/-} mice testis showed intensive β -galactosidase signal within the seminiferous tubules, but not on the Leydig cells or other interstitial tissue between tubules (Fig. 1D). Inside the seminiferous tubules, β -galactosidase activity was detected specifically on spermatocytes and spermatids. No signal was detected on the supporting seminiferous epithelium sertoli cells (Fig. 1D). On the other hand, *Faap20* expression in ovaries of 2 month-old *Faap20*^{+/-} mice was strictly observed in the small developmental primordial and primary follicles (Fig. 1D). These results indicate that *Faap20* expression is gametogenesis specific, mainly in the spermatocytes and spermatids or primordial and primary follicles, all of which are the major meiosis-stage haploid cells during spermatogenesis or oocytogenesis, respectively.

Loss of *Faap20* leads to mild FA-like cellular phenotypes

Since G₂M arrest and mitomycin C (MMC) hypersensitivity are the cellular hallmarks of FA cells,¹⁷⁻¹⁹ we generated primary murine embryonic fibroblasts (MEFs) from E11.5 wild-type and *Faap20*^{-/-} embryos and analyzed the cell cycle and survival in respond to MMC treatment. Cell cycle profiling revealed that there was a significant accumulation of G₂M phase in *Faap20*^{-/-} cells both at baseline and upon MMC treatment compared to wild-type MEFs (Fig. 2A). These data indicate that *Faap20*^{-/-} cells undergo G₂M arrest at both steady and stressed stages.

Because FAAP20 interacts with FANCA and regulates the FA core complex,¹¹⁻¹⁴ we compared MMC sensitivity of primary MEFs from *Faap20*^{-/-} mice to those from *Fanca*^{-/-} or *Fancc*^{-/-} mice. Cell cycle analysis of cells subjected to 100 nM MMC treatment for 24

h showed that *Faap20*^{-/-} cells underwent less severe G₂M arrest than *Fanca*^{-/-} or *Fancc*^{-/-} cells (Fig. 2B). Consistently, *Faap20*^{-/-} cells exhibited less apoptosis (Fig. 2C) and a better survival rate (Fig. 2D) than *Fancc*^{-/-} cells in response to MMC treatment. Taken together, these results indicate that deletion of *Faap20* leads to a milder cellular phenotype compared to loss of the FA core complex in the context of MMC sensitivity.

It has been shown that FA-deficient mouse HSC and progenitor cells are defective in hematopoietic repopulation.²⁰⁻²⁶ To assess the effect of *Faap20* loss on HSC function, we performed competitive long-term reconstitution assays using bone marrow cells from *Faap20*^{-/-}, *Fanca*^{-/-} or *Fancc*^{-/-} mice and their littermate controls. Although less robust than wild-type controls, *Faap20*^{-/-} HSCs showed milder defect in long-term multi-lineage reconstitution for myeloid, B, and T cells in lethally irradiated recipient mice, as compared to bone marrow HSCs from *Fanca*^{-/-} or *Fancc*^{-/-} mice (Fig. 2E). We also performed colony-forming assays to evaluate the effect of *Faap20* deficiency on the proliferation of hematopoietic progenitor cells in the absence of functional bone marrow niche and under condition of DNA damage by MMC. Again, loss of *Faap20* resulted in a milder defect than deficiency in the FA core complex (i.e. *Fanca*^{-/-} or *Fancc*^{-/-}) in the colony forming capacity of hematopoietic precursors in response to MMC (Fig. 2F). Collectively, these results provide in vivo evidence that deletion of the murine *Faap20* gene induces mild FA-like cellular phenotypes.

***Faap20*^{-/-} mice are susceptible to MMC-induced pancytopenia**

BM failure does not occur spontaneously but can be induced by DNA damage or other stresses in some FA mouse models.^{20,25} We next examined whether MMC could induce BM failure in *Faap20*^{-/-} mice. No grossly difference was observed between *Faap20*^{-/-} mice and wild-type littermates in hematological parameters in the peripheral blood (Fig. 3A& S2C), BM cellularity (Fig. 3B), and lineage differentiation (Fig. 3C) at the steady stage. However, two weeks after acute exposure to one single injection of 8 mg/kg MMC, *Faap20*^{-/-} mice showed severe pancytopenia, with significantly reduced BM cellularity, Hb, PLT (Fig. 3A-B). In the MMC-treated cohorts, we observed more severe reduction in erythroid lineage than myeloid/lymphoid lineage between *Faap20*^{-/-} and wild-type mice (Fig. 3C). Consequently, all MMC-treated *Faap20*^{-/-} mice died within 15 days, mostly due to BM failure (Fig. 3D). Thus, these results indicate that like FA deficiency, loss of *Faap20* renders mice susceptible to MMC-induced pancytopenia.

MMC induces specific defect in early erythroid progenitor and MEP compartments in *Faap20*^{-/-} mice

The observation that MMC treatment dramatically reduced RBC and erythroid lineage prompted us to analyze the erythroid differentiation program in *Faap20*^{-/-} mice, using the erythroid progenitor markers CD71 and TER119 to identify distinct cell populations at specific stages of erythrocyte differentiation (Fig. 4A). We found that MMC induced significant reduction of basophilic erythroblasts (R2, 77.6%, p<0.01) and late basophilic and chromatophilic erythroblasts (R3, 78.5%, p<0.001), but not orthochromatophilic erythroblasts (R4) in *Faap20*^{-/-} mice compared to wild-type littermate controls (Fig. 4A,

B). In contrast, we observed a compensative enrichment in the more mature reticulocyte (R5) population in MMC-treated *Faap20*^{-/-} mice (Fig. 4A, B).

We next examined the effect of MMC on the upstream progenitor compartments in *Faap20*^{-/-} mice. We found that MMC induced a significant percentage decrease in common myeloid progenitors (CMPs) and megakaryocyte-erythrocyte progenitors (MEPs) but a compensatory increase in granulocyte-macrophage progenitors (GMPs) in the LK (Lin-cKit⁺) population in *Faap20*^{-/-} mice compared to WT littermate controls (Fig. 4C, D). A significant reduction of common lymphoid progenitors (CLPs) was also observed in MMC-treated *Faap20*^{-/-} mice (Fig. 4E). Thus, it appears that *Faap20* deficiency affects CMPs and MEPs more than GMPs in the context of MMC sensitivity. In agreement with a differential functional role of *Faap20* in lineage progenitors, we found that *Faap20* expression was significantly higher in CMPs and MEPs than in GMPs (Fig. S5).

***Faap20*^{-/-} HSPCs display aberrant cell cycle pattern under chronic MMC stress**

To understand the mechanism underlying genotoxic stress-induced pancytopenia in *Faap20*^{-/-} mice, we performed cell cycle analysis on the HSPCs in *Faap20*^{-/-} mice. Because acute high dose MMC treatment on the *Faap20*^{-/-} mice caused almost complete bone marrow HSPCs depletion with not enough cells for FACS analysis and chronic MMC stress may reflect more physiologic challenges from the environment, the *Faap20*^{-/-} and WT control mice were subject to weekly injection with low dosage MMC (0.8mg/kg) in accordance to the published protocol for FA mice^{20,27}. The pancytopenia phenotype was observed in *Faap20*^{-/-} mice around 6-8 weeks, as evidenced by a significant reduction in the number of WBC, RBC, platelets counts, and Hb level in *Faap20*^{-/-} mice in comparison with WT mice (Fig. 5A). Again, MMC induced a significant decrease in the LK (Lin-cKit⁺) compartment, particularly MEPs of *Faap20*^{-/-} mice, as compared with those of WT mice (Fig. 5B). In addition, we observed a progressive reduction of phenotypic BM HSCs (LSK CD150⁺ CD48⁻; SLAM) in MMC-treated *Faap20*^{-/-} mice (Fig. 5D). Cell cycle analysis with PI and Ki67 staining showed aberrant cell cycle pattern characterized by decreased quiescent (G₀) or increased cycling (S/G₂M) cells in CMPs, MEPs and SLAMs populations of *Faap20*^{-/-} mice after 8 weeks of MMC treatment (Fig. 5C, E). Thus, these results suggest that low level of chronic genotoxic stress may cause replicative exhaustion of *Faap20*^{-/-} HSPCs, which may be one major mechanism responsible for HSPC depletion and pancytopenia phenotype in MMC-treated *Faap20*^{-/-} mice.

Possible dominant effect of FANCA protein in the interaction between FAAP20 and FANCA in response to MMC

To study the relationship between *Faap20* and *Fanca*, we generated *Faap20*^{-/-}*Fanca*^{-/-} double knockout (dKO) mice. Analysis of donor-derived total or lineage-specific repopulation in the peripheral blood show no significant difference between the *Fanca*^{-/-} and *Faap20*^{-/-}*Fanca*^{-/-} recipient cohorts (Fig. 6A). The repopulating capacity of *Fanca*^{-/-} BM HSCs in lethally irradiated recipient mice was not further reduced by a simultaneous *Faap20* deficiency. Also, colony-forming assays showed that loss of *Faap20* did not aggravate the extent of MMC effect on *Fanca*^{-/-} BM HSPC proliferation *in vitro* (Fig. 6B). Consistent with previous reports in human cell lines,^{12,13} we observed a lower

level of FAAP20 protein in *Fanca*^{-/-} MEFs than in wild-type cells (Fig. 6C), supporting the notion that FANCA stabilizes FAAP20. These data imply a possible dominant effect of FANCA over FAAP20.

To further understand the mechanistic role of FAAP20 in the FA pathway, we performed western blot and immunostaining on the MEFs and lineage-negative cells derived from *WT*, *Faap20*^{-/-}, *Fanca*^{-/-}, or *Fancd2*^{-/-} mice, with or without MMC treatment (Fig.S6 & S7). We observed partial FANCD2 monoubiquitination in the *Faap20*^{-/-} MEFs in comparison to non-FANCD2 ubiquitination in *Fanca*^{-/-} MEFs. In addition, less intensive phospho-Histone H2A.X (Ser139) signal was detected in the *Faap20*^{-/-} cells in comparison to *Fanca*^{-/-} or *Fancd2*^{-/-} cells, indicating less DNA damage. These data suggest that the FA complex is not completely disrupted in the absence of FAAP20.

Discussion

Multiple Fanconi Anemia (FA) mouse models have been generated to study the role of FA proteins in growth and development.^{15,16,27-32} These FA mice generally exhibit decreased fertility with abnormal germ cell development and increased DNA cross-linker sensitivity.^{16,27,30} The FA mice also show hematopoietic stem cell (HSPC) dysfunction upon transplantation and develop bone marrow failure after MMC injection.^{20,24,26} To explore the *in vivo* function of the newly discovered FAAP20 protein, we have characterized the *Faap20*^{-/-} mice with the exon1c and exon2 of the *Faap20* gene replaced by a β -galactosidase gene. The *Faap20*^{-/-} mice display similar features of other FA knockout mouse models. For example, similar to *Fanca*^{-/-}, *Fancc*^{-/-}, *Fancg*^{-/-} and *Fancd2*^{-/-} mice^{16,27,30,31}, *Faap20*^{-/-} mice show defects in reproductive organs, hematopoietic repopulation and cellular resistance to DNA cross-linking agent MMC. Interestingly, *Faap20*^{-/-} mice exhibit milder FA-like phenotypes than mice deficient for the FA core complex components such as FANCA or FANCC. For instance, although inter-cross of *Faap20*^{-/-} mice exhibited significantly reduced litter sizes, the *Fanca*^{-/-}, *Fancc*^{-/-} and *Fancd2*^{-/-} mice are completely infertile. In addition, BM HSC and progenitor cells from *Fanca*^{-/-} or *Fancc*^{-/-} mice are more sensitive to replicative stress induced by transplantation or genotoxic stress resulting from DNA cross-links than those from *Faap20*^{-/-} mice. Our results suggest that loss of *Faap20* may not completely disrupt the formation of the FA core complex. Thus, partial monoubiquitination of FANCD2 and less DNA damage in the *Faap20*^{-/-} cells may be responsible for the mild FA-like phenotypes we observed in the *Faap20*^{-/-} mice (Fig.S6 & S7). In supporting this notion, previously study indicates that residual monoubiquitination of FANCD2 was detected in FAAP20-deficient human cell lines.¹²

Another interesting finding of the current study is the observation that the expression of mouse *Faap20* is regulated in developmental and tissue-specific manner. We observed high levels of *Faap20* expression in stages of E11.5 embryos, suggesting that a role of *Faap20* during the early development. Consistent with this, it has been reported that FANCA is also expressed in E7.5 and E11.5 embryos,¹⁵ and that 60–75% of FA patients were born with congenital defects, prenatal lethality and growth retardation.^{4,33,34} Interestingly, *Faap20* is specifically expressed in the hippocampus and cortex region in the brain (Fig. S3C).

Relevant to this, it is noteworthy that some FA patients display central nervous system symptoms, including increased fluid in the center of the brain (hydrocephalus) or an unusually small head size (microcephaly).³⁵⁻³⁷ The function of *Faap20* in hippocampus and cortex of the brain remains to be investigated. Also, the *Faap20* expression was observed in the cyst of intestine tissue and part of the uterus.

The highest level of *Faap20* expression was detected in the testes and ovaries of adult mice. This is consistent with the reproductive defects observed in *Faap20*^{-/-} mice. Similarly, FANCA and FANCD2 are also highly expressed in the testes and *Fanca* or *Fancd2* deficiency causes reproductive defects in mice.^{15,23} Furthermore, we observed intensive β -galactosidase signal specifically in spermatocytes and spermatids of testes and in the small primordial and primary follicles of ovaries (Fig. 2D). This is the stage during gametogenesis when meiotic recombination results in formation and repair of DNA double-stranded breaks. In addition, it has been shown that increased FANCA expression is restricted to mid- to late-pachytene spermatocytes.¹⁵ Collectively, these observations suggested that FAAP20 may function in meiotic recombination during spermatogenesis and oocytogenesis.

Previously studies suggested that FAAP20 might also possess DNA repair function outside of the FA pathway, as the ubiquitin-binding activity elicited by the UBZ domain of FAAP20 is independent of the FAAP20-FANCA interaction.¹³ Based on this information, we hypothesized that deletion of *Faap20* in *Fanca*^{-/-} mice might exhibit a more severe phenotype than *Fanca*^{-/-} mice. However, our results show that loss of *Faap20* did not aggravate *Fanca*^{-/-} phenotype and FAAP20 protein level was almost negligible in *Fanca* null MEFs by western blot (Fig. 6). In addition, previously studies indicate that FAAP20 could bind to ubiquitinated Rev1 or histone H2A then trigger the recruitment of FA core complex to the ICLs site, suggesting that FAAP20 may function downstream of the FA core complex.^{11,14} In this context, we propose a possible dominant effect of the FANCA protein in the interaction between FANCA and FAAP20 during ICL repair.

Interestingly, we observed differential effects of MMC-induced genotoxic stress on specific lineages of *Faap20*^{-/-} BM progenitors. Both high-dose acute and low-dose chronic exposure of *Faap20*^{-/-} mice to MMC induced severe pancytopenia, most likely resulting from injuries to HSPCs especially the erythroid progenitors and their upstream MEPs (Figs. 4, 5). MMC-induced BM failure has been reported in *Fancg*^{-/-} and *Fancc*^{-/-} mice.^{20,27} However, the cellular mechanism responsible for this hallmark phenotype was not further investigated. In this study, we showed that the LKs and SLAM populations in MMC-treated *Faap20*^{-/-} mice displayed an aberrant cell cycle pattern featuring decreased quiescent (G₀) and increased cycling (S/G₂M) cells (Fig. 5), typical of replicative exhaustion in these HSPCs. It is possible that the increased MMC injury observed in erythroid progenitors and MEPs over GMPs cells was due to the fact that erythroid progenitors and MEPs cycle more rapidly than myeloid and GMPs do.³⁸ Consistently, we detected higher levels of *Faap20* expression in the erythroid progenitors, CMPs and MEPs compared with mature myeloid (Mac1+Gr1+) cells and GMPs (Fig. S5). A recent clinical study of FA patients identifies dyserythropoiesis and dysmegakaryopoiesis as the most common morphologic abnormalities,⁵ further corroborating the notion that the erythroid cells and their precursor MEPs may be more vulnerable to DNA damage stress than other lineages in FA. Our results

are consistent with the role of FAAP20 in cell survival following MMC-induced DNA damage and replicative stress. In this context, the *Faap20* mouse model may be a useful tool for studying mechanisms underlying the pathophysiology of FA BM failure.

Supplementary Material

Refer to Web version on PubMed Central for supplementary material.

Acknowledgements

We thank Dr. Madeleine Carreau (Laval University) for the *Fanca*^{+/-} mice, Dr. Manuel Buchwald (Hospital for Sick Children, University of Toronto) for the *Fancc*^{+/-} mice, the Transgenic Animal and Genome Editing Core (Cincinnati Children's Hospital Medical Center) for IVF service, and the Comprehensive Mouse and Cancer Core of the Cincinnati Children's Research Foundation (Cincinnati Children's Hospital Medical Center) for bone marrow transplantation service. This investigation was supported by NIH grants R01 HL076712, R01 CA157537 and T32 HL091805. Q.P. is supported by a Leukemia and Lymphoma Scholar award.

References

2. Bagby GC Jr. Genetic basis of Fanconi anemia. *Curr Opin Hematol.* 2003; 10(1):68–76. [PubMed: 12483114]
2. Auerbach AD, Allen RG. Leukemia and preleukemia in Fanconi anemia patients. A review of the literature and report of the International Fanconi Anemia Registry. *Cancer Genet Cytogenet.* 1991; 51(1):1–12. [PubMed: 1984836]
3. Tischkowitz M, Dokal I. Fanconi anaemia and leukaemia - clinical and molecular aspects. *Br J Haematol.* 2004; 126(2):176–191. [PubMed: 15238138]
4. Kutler DI, Singh B, Satagopan J, et al. A 20-year perspective on the International Fanconi Anemia Registry (IFAR). *Blood.* 2003; 101(4):1249–1256. [PubMed: 12393516]
5. Cioc AM, Wagner JE, MacMillan ML, DeFor T, Hirsch B. Diagnosis of myelodysplastic syndrome among a cohort of 119 patients with fanconi anemia: morphologic and cytogenetic characteristics. *Am J Clin Pathol.* 2010; 133(1):92–100. [PubMed: 20023263]
6. Muller LU, Williams DA. Finding the needle in the hay stack: hematopoietic stem cells in Fanconi anemia. *Mutat Res.* 2009; 668(1-2):141–149. [PubMed: 19508850]
7. Garaycochea JI, Patel KJ. Why does the bone marrow fail in Fanconi anemia? *Blood.* 2014; 123(1):26–34. [PubMed: 24200684]
8. Kim H, D'Andrea AD. Regulation of DNA cross-link repair by the Fanconi anemia/BRCA pathway. *Genes Dev.* 2012; 26(13):1393–1408. [PubMed: 22751496]
9. Crossan GP, Patel KJ. The Fanconi anaemia pathway orchestrates incisions at sites of crosslinked DNA. *J Pathol.* 2012; 226(2):326–337. [PubMed: 21956823]
10. Kee Y, D'Andrea AD. Expanded roles of the Fanconi anemia pathway in preserving genomic stability. *Genes Dev.* 2010; 24(16):1680–1694. [PubMed: 20713514]
11. Yan Z, Guo R, Paramasivam M, et al. A ubiquitin-binding protein, FAAP20, links RNF8-mediated ubiquitination to the Fanconi anemia DNA repair network. *Mol Cell.* 2012; 47(1):61–75. [PubMed: 22705371]
12. Leung JW, Wang Y, Fong KW, Huen MS, Li L, Chen J. Fanconi anemia (FA) binding protein FAAP20 stabilizes FA complementation group A (FANCA) and participates in interstrand cross-link repair. *Proc Natl Acad Sci U S A.* 2012; 109(12):4491–4496. [PubMed: 22396592]
13. Ali AM, Pradhan A, Singh TR, et al. FAAP20: a novel ubiquitin-binding FA nuclear core-complex protein required for functional integrity of the FA-BRCA DNA repair pathway. *Blood.* 2012; 119(14):3285–3294. [PubMed: 22343915]
14. Kim H, Yang K, Dejsuphong D, D'Andrea AD. Regulation of Rev1 by the Fanconi anemia core complex. *Nat Struct Mol Biol.* 2012; 19(2):164–170. [PubMed: 22266823]

14. Wong JC, Alon N, McKerlie C, Huang JR, Meyn MS, Buchwald M. Targeted disruption of exons 1 to 6 of the Fanconi Anemia group A gene leads to growth retardation, strain-specific microphthalmia, meiotic defects and primordial germ cell hypoplasia. *Hum Mol Genet.* 2003; 12(16):2063–2076. [PubMed: 12913077]
16. Chen M, Tomkins DJ, Auerbach W, et al. Inactivation of Fac in mice produces inducible chromosomal instability and reduced fertility reminiscent of Fanconi anaemia. *Nat Genet.* 1996; 12(4):448–451. [PubMed: 8630504]
17. Seyschab H, Friedl R, Sun Y, et al. Comparative evaluation of diepoxybutane sensitivity and cell cycle blockage in the diagnosis of Fanconi anemia. *Blood.* 1995; 85(8):2233–2237. [PubMed: 7718895]
18. Heinrich MC, Hoatlin ME, Zigler AJ, et al. DNA cross-linker-induced G2/M arrest in group C Fanconi anemia lymphoblasts reflects normal checkpoint function. *Blood.* 1998; 91(1):275–287. [PubMed: 9414295]
19. Akkari YM, Bateman RL, Reifsteck CA, D'Andrea AD, Olson SB, Grompe M. The 4N cell cycle delay in Fanconi anemia reflects growth arrest in late S phase. *Mol Genet Metab.* 2001; 74(4): 403–412. [PubMed: 11749045]
20. Carreau M, Gan OI, Liu L, et al. Bone marrow failure in the Fanconi anemia group C mouse model after DNA damage. *Blood.* 1998; 91(8):2737–2744. [PubMed: 9531583]
21. Haneline LS, Gobbett TA, Ramani R, et al. Loss of FancC function results in decreased hematopoietic stem cell repopulating ability. *Blood.* 1999; 94(1):1–8. [PubMed: 10381491]
22. Haneline LS, Li X, Ciccone SL, et al. Retroviral-mediated expression of recombinant FancC enhances the repopulating ability of FancC^{-/-} hematopoietic stem cells and decreases the risk of clonal evolution. *Blood.* 2003; 101(4):1299–1307. [PubMed: 12393504]
23. Parmar K, Kim J, Sykes SM, et al. Hematopoietic stem cell defects in mice with deficiency of Fancd2 or Usp1. *Stem Cells.* 2010; 28(7):1186–1195. [PubMed: 20506303]
24. Li X, Le Beau MM, Ciccone S, et al. Ex vivo culture of FancC^{-/-} stem/progenitor cells predisposes cells to undergo apoptosis, and surviving stem/progenitor cells display cytogenetic abnormalities and an increased risk of malignancy. *Blood.* 2005; 105(9):3465–3471. [PubMed: 15644418]
25. Milsom MD, Lee AW, Zheng Y, Cancelas JA. FancA^{-/-} hematopoietic stem cells demonstrate a mobilization defect which can be overcome by administration of the Rac inhibitor NSC23766. *Haematologica.* 2009; 94(7):1011–1015. [PubMed: 19491337]
26. Navarro S, Meza NW, Quintana-Bustamante O, et al. Hematopoietic dysfunction in a mouse model for Fanconi anemia group D1. *Mol Ther.* 2006; 14(4):525–535. [PubMed: 16859999]
27. Koomen M, Cheng NC, van de Vrugt HJ, et al. Reduced fertility and hypersensitivity to mitomycin C characterize Fancg/Xrcc9 null mice. *Hum Mol Genet.* 2002; 11(3):273–281. [PubMed: 11823446]
28. Bakker ST, de Winter JP, te Riele H. Learning from a paradox: recent insights into Fanconi anaemia through studying mouse models. *Dis Model Mech.* 2013; 6(1):40–47. [PubMed: 23268537]
29. Parmar K, D'Andrea A, Niedernhofer LJ. Mouse models of Fanconi anemia. *Mutat Res.* 2009; 668(1-2):133–140. [PubMed: 19427003]
30. Cheng NC, van de Vrugt HJ, van der Valk MA, et al. Mice with a targeted disruption of the Fanconi anemia homolog FancA. *Hum Mol Genet.* 2000; 9(12):1805–1811. [PubMed: 10915769]
31. Houghtaling S, Timmers C, Noll M, et al. Epithelial cancer in Fanconi anemia complementation group D2 (Fancd2) knockout mice. *Genes Dev.* 2003; 17(16):2021–2035. [PubMed: 12893777]
32. Bakker ST, van de Vrugt HJ, Rooimans MA, et al. Fancm-deficient mice reveal unique features of Fanconi anemia complementation group M. *Hum Mol Genet.* 2009; 18(18):3484–3495. [PubMed: 19561169]
33. Antonio, Casado J.; Callen, E.; Jacome, A., et al. A comprehensive strategy for the subtyping of patients with Fanconi anaemia: conclusions from the Spanish Fanconi Anemia Research Network. *J Med Genet.* 2007; 44(4):241–249. [PubMed: 17105750]
34. Ameziane N, Errami A, Leveille F, et al. Genetic subtyping of Fanconi anemia by comprehensive mutation screening. *Hum Mutat.* 2008; 29(1):159–166. [PubMed: 17924555]

35. Porteous ME, Cross I, Burn J. VACTERL with hydrocephalus: one end of the Fanconi anemia spectrum of anomalies? *Am J Med Genet.* 1992; 43(6):1032–1034. [PubMed: 1415330]
36. Alter BP. Hydrocephalus in Fanconi anemia. *Am J Med Genet.* 1993; 45(6):785. [PubMed: 8456865]
37. Cox PM, Gibson RA, Morgan N, Brueton LA. VACTERL with hydrocephalus in twins due to Fanconi anemia (FA): mutation in the FAC gene. *Am J Med Genet.* 1997; 68(1):86–90. [PubMed: 8986283]
38. Matarraz S, Teodosio C, Fernandez C, et al. The proliferation index of specific bone marrow cell compartments from myelodysplastic syndromes is associated with the diagnostic and patient outcome. *PLoS One.* 2012; 7(8):e44321. [PubMed: 22952954]

Key Points

Deletion of *Faap20* in mice causes a mild FA-like phenotype. *Faap20*^{-/-} mice show reproductive defect and are susceptible to genotoxic stress induced bone marrow failure resulting from depletion of early hematopoietic progenitors.

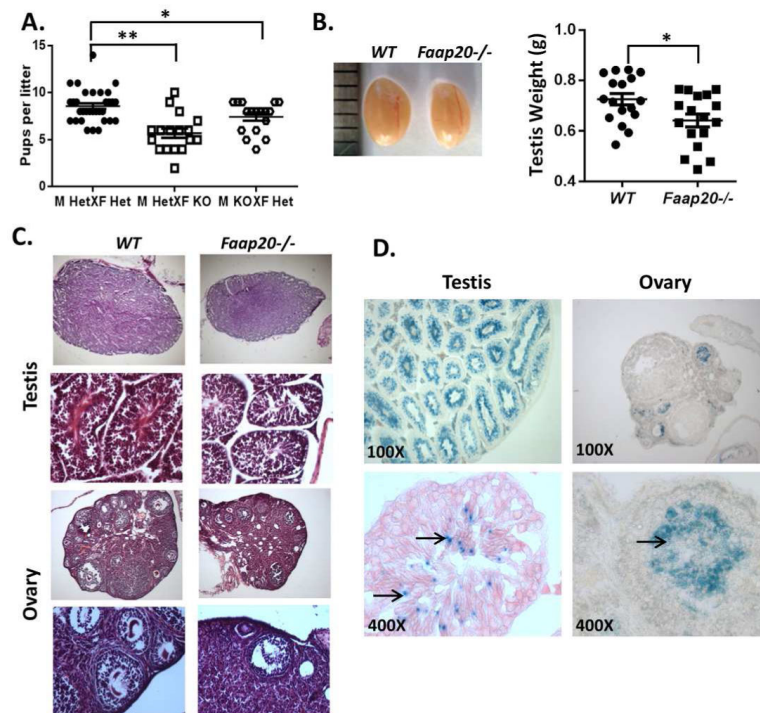


Figure 1. Impaired fertility and gonadal development in *Faap20*^{-/-} mice

(A) *Faap20*^{-/-} mice exhibit reduced reproduction ability. Reproductive performance of 4 pairs of mice per group was followed over time. *Faap20*^{-/-} (KO) mice were crossed with heterozygote (Het) mice. Heterozygotes (Het) and heterozygotes (Het) crossing was used as controls. (B) The testes of *Faap20*^{-/-} mice are smaller than their wild type littermates. Photograph show testis from wild type (left) male and *Faap20*^{-/-} littermate (right). (C) H&E stained testis and ovary sections from 2 month-old *Faap20*^{-/-} and wild type littermates show developmental defect in gonads. All stages of spermatogenesis are seen in the wild-type adult testis. *Faap20*^{-/-} testis show seminiferous tubules with scattered sertoli cells and decreased number of spermatocytes and spermatids. Many follicles with oocytes at various stages of development can be seen in the wild type ovary. The *Faap20*^{-/-} ovary is smaller in comparison to the wild type ovary with reduced number of follicles (Magnification 50X, 100X, 200X). (D) β-Gal staining of testis and ovary sections from 2 month-old *Faap20*^{+/-} mice show cell type specific expression of FAAP20. There was no specific staining in epithelial and sertoli cells, but strong blue staining was seen in the spermatocytes and spermatids (arrows) in testis. In ovary section, the β-Gal signal was detected only in the follicles area (arrow). (Magnification 100X, 400X).

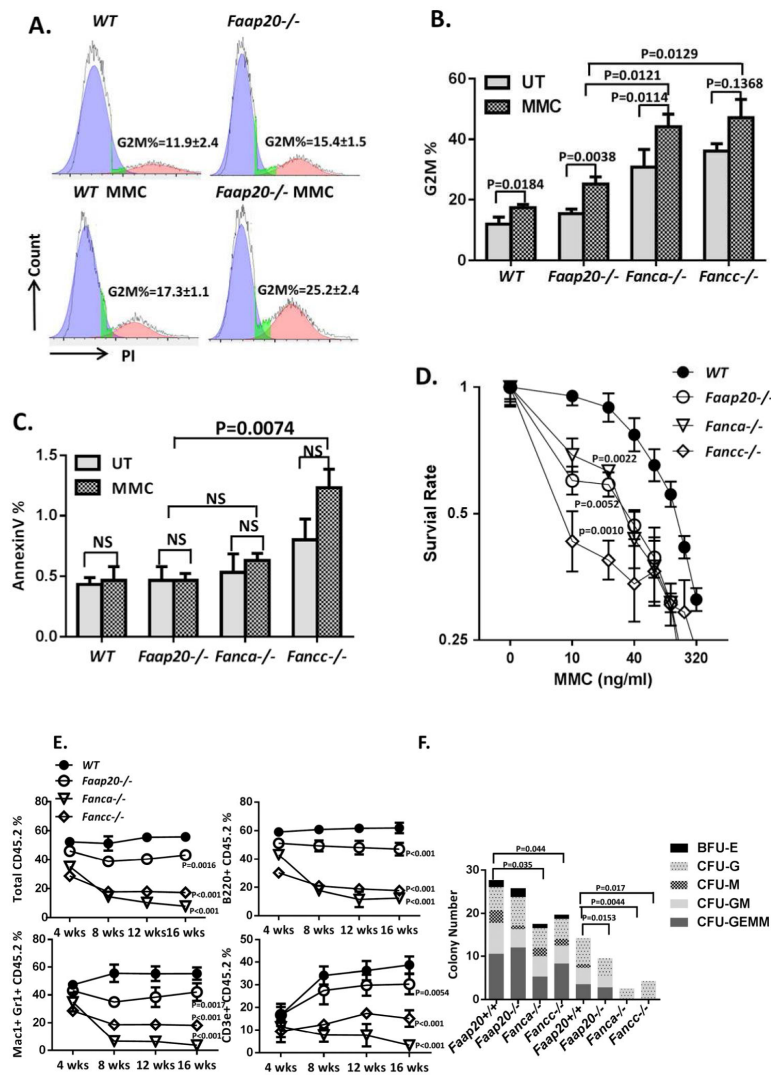


Figure 2. *Faap20*^{-/-} MEFs and bone marrow cells show typical FA features, but with milder phenotypes in comparison to *Fanca*^{-/-} or *Fanc*^{-/-} cells

(A) *Faap20*^{-/-} MEFs exhibit increased G₂M arrest before and after MMC treatment. Wild type and *Faap20*^{-/-} MEFs cells cultured with or without MMC (100 nM) for 24 hours were analyzed by propidium iodide (PI) DNA content staining. The G₂M phase percentage was quantified by cell cycle tools in FlowJo. (B) *Faap20*^{-/-}, *Fanc*^{-/-} and *Fanca*^{-/-} MEFs show increased G₂M phase than wild type MEFs before and after MMC treatment. The G₂M arrest in *Fanc*^{-/-} and *Fanca*^{-/-} MEFs was more severe than *Faap20*^{-/-} MEFs. Different genotypes of MEFs were stained for PI, and analyzed with FACS 24 hours after MMC treatment. Results were expressed as the percentages of G₂M phase cells treated with (MMC) or without (UT) MMC. (C) Cell apoptosis rate was increased in *Fanc*^{-/-} MEFs, but not in *Faap20*^{-/-} and *Fanca*^{-/-} MEFs. Different genotype of MEFs were stained for Annexin V, and analyzed with FACS 24 hours after MMC treatment. (D) *Faap20*^{-/-}, *Fanc*^{-/-} and *Fanca*^{-/-} MEFs show reduced survival rate than wild type MEFs after MMC treatment. *Fanc*^{-/-} MEFs is more sensitive than the *Faap20*^{-/-} and *Fanca*^{-/-} MEFs. The MEFs were plated after treatment with or without MMC for 24 hours

and colonies were counted after 8 days. Data represent percentage survival, comparing each dose to untreated cells. (E) *Faap20*^{-/-} bone marrow show reduced long-term repopulating activity in vivo, but not as severe as the *Fanca*^{-/-} or *Fancc*^{-/-} bone marrow. Irradiated CD45.1+ recipient mice were competitively reconstituted with 1×10⁶ CD45.2+ bone marrow cells from wild type, *Faap20*^{-/-}, *Fanca*^{-/-} or *Fancc*^{-/-} along with 1×10⁶ CD45.1+ recipient bone marrow cells. Donor-derived total (CD45.2+), B cell (B220+), myeloid cell (Mac1+ Gr1+), and T cell (CD3e+) engraftment in peripheral blood of transplanted recipients were analyzed each month for 4 months. Each line represents average donor cell reconstitution levels from 3 independent experiments with 4-6 recipients/experiment. (F) Decreased colony-forming activity of *Faap20*^{-/-} bone marrow progenitors under genotoxic condition. Total colony numbers formed by wild type, *Faap20*^{-/-}, *Fanca*^{-/-} or *Fancc*^{-/-} BM cells treated with (MMC) or without (UT) MMC are shown. BFU-E: Burst-Forming Unit-Erythroid; CFU-GM: Colony-Forming Unit-Granulocyte/Macrophage; CFU-G: Colony Forming Unit-Granulocyte; CFU-M: Colony-Forming Unit-Macrophage; CFU-GEMM: Colony-Forming Unit-Granulocyte/Erythrocyte/Macrophage/Megakaryocyte. Data represent mean ± SD of 3 experiments with four replicates each.

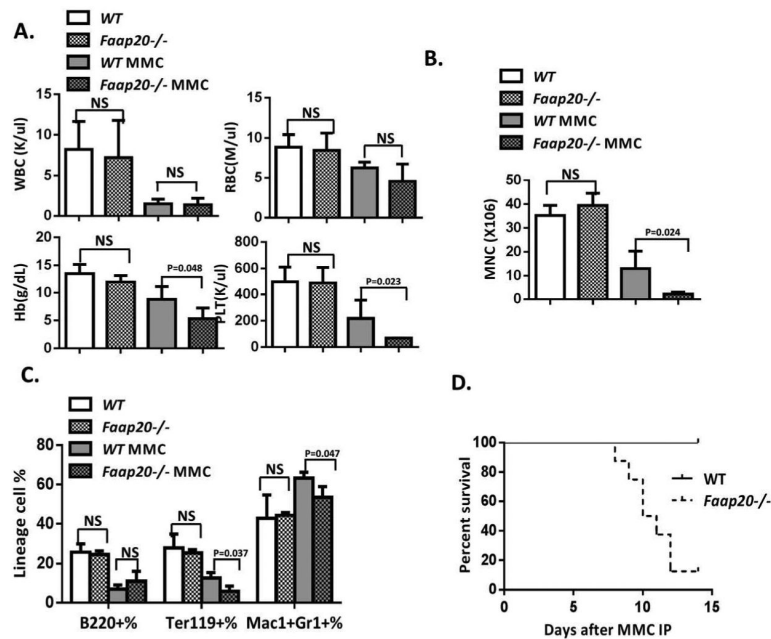


Figure 3. *Faap20*^{-/-} mice are vulnerable to MMC-induced pancytopenia

Faap20^{-/-} mice and their wild type littermates at 6-8 weeks of age were injected with 8mg/kg MMC. PBS injected *Faap20*^{-/-} or wild type mice were used as controls. Mice were analyzed 8 days after injection. (A) Hematological parameters of peripheral blood cells show bone marrow failure in *Faap20*^{-/-} mice after MMC injection. Data represent mean \pm SD of two to four independent experiments with more than three mice for each group per experiment. (B) Reduced bone marrow cellularity in *Faap20*^{-/-} mice after MMC treatment. Total bone marrow mononuclear cells from two femurs plus two tibias of individual animals ($n > 4$) of indicated genotypes and treatment were isolated and counted. (C) Bone marrow cells were divided into individual lineage compartments according to cell surface markers using flow cytometric analysis. Numbers represent percentages of the B cells (B220+), erythroid (Ter119+) or myeloid (Mac1+Gr1+) lineage of bone marrow cells. (D) Survival of recipients ($n > 10$) was monitored by Kaplan-Meier curve method. Note that *Faap20*^{-/-} mice died at around 8-14 days after MMC injection.

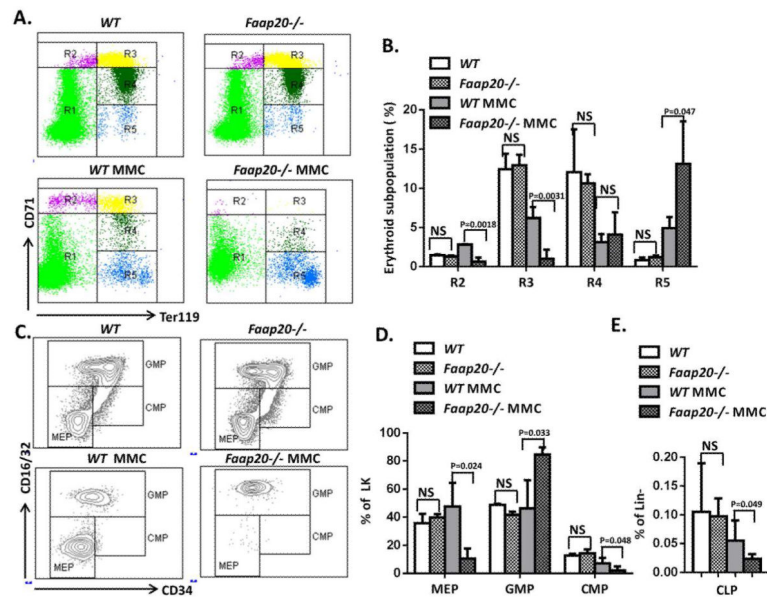


Figure 4. Loss of *Faap20* induces early erythroid progenitors and MEPs ablation after MMC treatment

Faap20^{-/-} or wild type mice at 6-8 weeks of age were injected with one dose 8mg/kg MMC to induce the bone marrow failure. PBS injected *Faap20*^{-/-} or wild type mice were used as controls. Mice were analyzed 8 days after injection. (A) The early erythroid progenitors in *Faap20*^{-/-} mice were depleted after MMC exposure. Freshly dissociated bone marrow cells were labeled with CD71 and Ter119 mAb, and subjected to flow cytometric analysis. The five regions (R1 to R5) within a flow cytometry scatter plot contain distinct cell types found in the different stages of erythrocyte differentiation were selected as indicated. There are predominantly proerythroblasts in region R1, basophilic erythroblasts in region R2, late basophilic and chromatophilic erythroblasts in region R3, orthochromatophilic erythroblasts in region R4, and reticulocytes and erythrocytes in R5. (B) The percentages of R2-R5 cells in the bone marrow were quantitated from the data shown in (A). (C) Flow cytometry analysis show early progenitor depletion in *Faap20*^{-/-} mice treated with MMC. (D) Quantitation of CMPs, MEPs and GMPs in Lin-cKit⁺ (Lk) compartment. Data represent summary of more than three mice of each genotype from two independent experiments. (E) Quantitation of CLPs. Data represent summary of more than three mice of each genotype from two independent experiments.

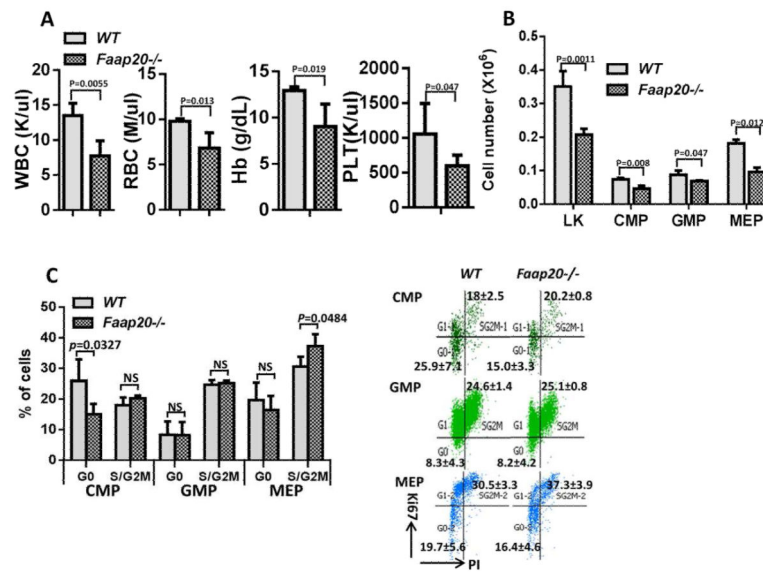


Figure 5. Aberrant cell cycle pattern of HSPCs in *Faap20*^{-/-} mice after chronic MMC stress
Faap20^{-/-} mice and their WT littermates at 6-8 weeks of age were injected with 0.8mg/kg MMC weekly. The mice were sacrificed and analyzed after 8 weeks of IP administration. (A) WBC, RBC, PLT counts and the Hb level in *Faap20*^{-/-} were significantly decreased compared to WT mice after 8 weeks of MMC treatment. (B) Decreased number of LKs and MPPs subpopulation in *Faap20*^{-/-} mice after MMC stress. (C) The CMPs and MEPs, but not GMPs population show aberrant cell cycle pattern in MMC-treated *Faap20*^{-/-} mice. The representative FACS graphs are shown on right. (D) The number of SLAM cells was progressively declined during long-term MMC stress in *Faap20*^{-/-} mice. (E) Increased cycling (S/G₂M) cells in the SLAM population of *Faap20*^{-/-} mice after 8 weeks of MMC injection. The representative FACS graphs are shown on right.

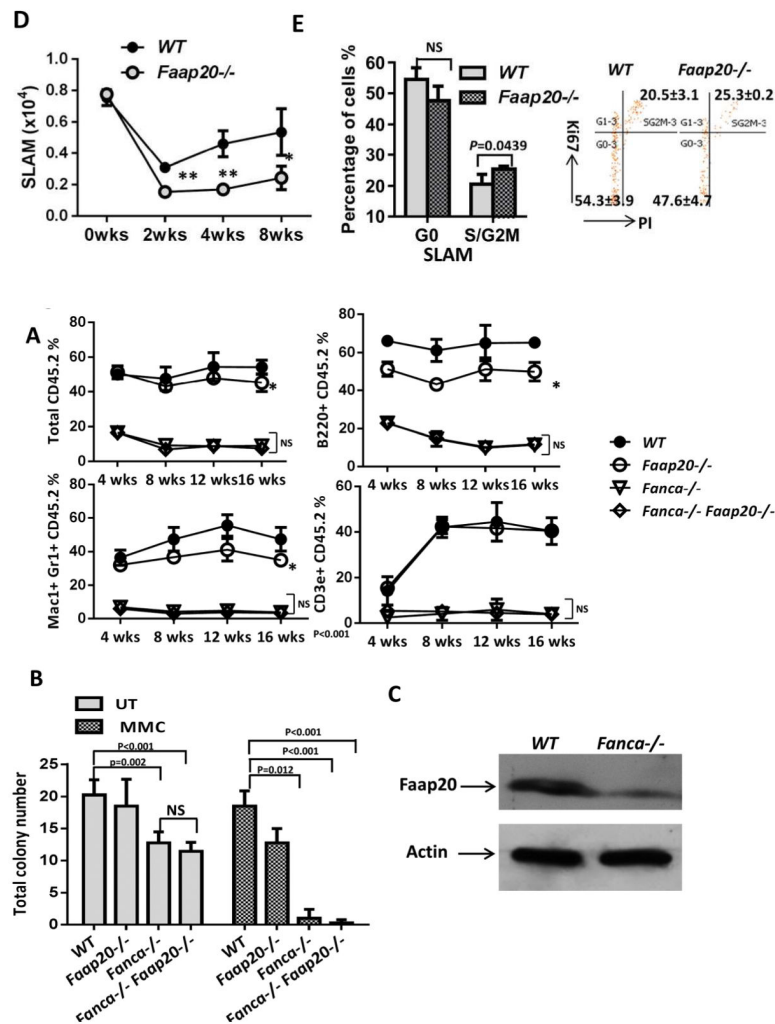


Figure 6. Loss of *Faap20* does not aggravate the bone marrow phenotype in *Fanca*^{-/-} mice
 (A) *Faap20* deficiency does not further compromise long-term repopulating activity of *Fanca*^{-/-} bone marrow HSPCs. Irradiated CD45.1⁺ recipient mice were competitively reconstituted with 1×10^6 CD45.2⁺ bone marrow cells from wild type, *Faap20*^{-/-}, *Fanca*^{-/-} or *Fanca*^{-/-}*Faap20*^{-/-} along with 1×10^6 CD45.1⁺ recipient bone marrow cells. Donor-derived total engraftment, B cell (B220⁺), myeloid cell (Mac1⁺ Gr1⁺), and T cell (CD3e⁺) engraftment in the peripheral blood of recipients were analyzed each month for 4 months. Each line represents average donor cell reconstitution levels from two independent experiments with 4-6 recipients per experiment. (B) Colony forming activity of WT, single KO (*Fanca*^{-/-} or *Faap20*^{-/-}), double KO (*Fanca*^{-/-}*Faap20*^{-/-}) bone marrow cells treated with (MMC) or without (UT) MMC. The double KO (*Fanca*^{-/-}*Faap20*^{-/-}) bone marrow cells did not exhibit reduced colony forming ability comparing to single *Fanca*^{-/-} KO bone marrow cells. Data represent mean \pm SD of two independent experiments with 4 replicates each genotype per experiment. (C) Immunoblotting show reduced expression levels of FAAP20 in *Fanca*^{-/-} MEFs cells.